World Journal of
Gastroenterology

WORLD JOURNAL of Gastroenterology

Contents

Contents

ABOUT COVER

Editorial board member of *World Journal of Gastroenterology*, Vito Annese, MD, PhD, Associate Professor, Chief Doctor, Department of Medical and Surgical Sciences, University Hospital Careggi, Florence 50139, Italy

AIMS AND SCOPE

The primary aim of *World Journal of Gastroenterology* (*WJG*, *World J Gastroenterol*) is to provide scholars and readers from various fields of gastroenterology and hepatology with a platform to publish high-quality basic and clinical research articles and communicate their research findings online.

  WJG mainly publishes articles reporting research results and findings obtained in the field of gastroenterology and hepatology and covering a wide range of topics including gastroenterology, hepatology, gastrointestinal endoscopy, gastrointestinal surgery, gastrointestinal oncology, and pediatric gastroenterology.

INDEXING/ABSTRACTING

The *WJG* is now indexed in Current Contents®/Clinical Medicine, Science Citation Index Expanded (also known as SciSearch®), Journal Citation Reports®, Index Medicus, MEDLINE, PubMed, PubMed Central, and Scopus. The 2019 edition of Journal Citation Report® cites the 2018 impact factor for *WJG* as 3.411 (5-year impact factor: 3.579), ranking *WJG* as 35th among 84 journals in gastroenterology and hepatology (quartile in category Q2). CiteScore (2018): 3.43.

RESPONSIBLE EDITORS FOR THIS ISSUE

Responsible Electronic Editor: *Yan-Liang Zhang*

Proofing Production Department Director: *Yun-Xiaojian Wu*

Responsible Editorial Office Director: *Ze-Mao Gong*

Basic Study

Sleeve gastrectomy ameliorates endothelial function and prevents lung cancer by normalizing endothelin-1 axis in obese and diabetic rats

Rexiati Ruze, Ya-Cheng Xiong, Jian-Wen Li, Ming-Wei Zhong, Qian Xu, Zhi-Bo Yan, Jian-Kang Zhu, Yu-Gang Cheng, San-Yuan Hu, Guang-Yong Zhang

ORCID number: Rexiati Ruze (0000-0002-0891-5307); Ya-Cheng Xiong (0000-0002-9642-5737); Jian-Wen Li (0000-0003-2035-8838); Ming-Wei Zhong (0000-0002-6548-550X); Qian Xu (0000-0002-6174-3348); Zhi-Bo Yan (0000-0003-3065-0621); Jian-Kang Zhu (0000-0001-5007-9528); Yu-Gang Cheng (0000-0003-3600-7047); San-Yuan Hu (0000-0002-0885-4292); Guang-Yong Zhang (0000-0001-5308-0129).

Author contributions: Zhang GY and Hu SY conceived of the experiments; Zhang GY and Li JW designed the experiments; Zhong MW, Zhu JK, and Cheng YG performed the literature research; Ruze R and Xiong YC carried out the experiments; Xu Q and Yan ZB performed the statistical analyses; Ruze R prepared the manuscript; Zhang GY gave final approval of the submitted and published versions.

Rexiati Ruze, Ya-Cheng Xiong, Qian Xu, Department of General Surgery, Shandong Provincial Qianfoshan Hospital, Shandong University, Jinan 250014, Shandong Province, China

Jian-Wen Li, Department of General Surgery, Ruijin Hospital, Shanghai Jiaotong University School of Medicine, Shanghai 200025, China

Ming-Wei Zhong, Jian-Kang Zhu, Yu-Gang Cheng, San-Yuan Hu, Guang-Yong Zhang, Department of General Surgery, The First Affiliated Hospital of Shandong First Medical University, Jinan 250014, Shandong Province, China

Zhi-Bo Yan, Department of General Surgery, Qilu Hospital of Shandong University, Jinan 250012, Shandong Province, China

Corresponding author: Guang-Yong Zhang, DSc, MD, PhD, Chief Doctor, Professor, Department of General Surgery, The First Affiliated Hospital of Shandong First Medical University, No. 16766, Jingshi Road, Jinan 250014, Shandong Province, China. guangyong-zhang@hotmail.com

Abstract

BACKGROUND

Previous evidence has implied that obesity is an independent risk factor for developing cancer. Being closely related to obesity, type 2 diabetes mellitus provides a suitable environment for the formation and metastasis of tumors through multiple pathways. Although bariatric surgeries are effective in preventing and lowering the risk of various types of cancer, the underlying mechanisms of this effect are not clearly elucidated.

AIM

To uncover the role and effect of sleeve gastrectomy (SG) in preventing lung cancer in obese and diabetic rats.

METHODS

SG was performed on obese and diabetic Wistar rats, and the postoperative transcriptional and translational alterations of the endothelin-1 (ET-1) axis in the lungs were compared to sham-operated obese and diabetic rats and age-matched healthy controls to assess the improvements in endothelial function and risk of developing lung cancer at the postoperative 4th, 8th, and 12th weeks. The risk was

also evaluated using nuclear phosphorylation of H2A histone family member X as a marker of DNA damage (double-strand break).

RESULTS
Compared to obese and diabetic sham-operated rats, SG brought a significant reduction to body weight, food intake, and fasting blood glucose while improving oral glucose tolerance and insulin sensitivity. In addition, ameliorated levels of gene and protein expression in the ET-1 axis as well as reduced DNA damage indicated improved endothelial function and a lower risk of developing lung cancer after the surgery.

CONCLUSION
Apart from eliminating metabolic disorders, SG improves endothelial function and plays a protective role in preventing lung cancer *via* normalized ET-1 axis and reduced DNA damage.

Key words: Sleeve gastrectomy; Lung cancer; Endothelin-1 axis; Endothelial dysfunction; DNA damage; Obesity

Core tip: To explore the potential mechanism of bariatric surgery to reduce the risk of cancer, sleeve gastrectomy (SG) was performed on obese and diabetic rats. As a result, with a disrupted endothelin-1 axis, sham-operated subjects manifested deteriorated endothelial function and an increased risk of developing cancer compared to the healthy controls. However, far more than improving glycometabolism, SG reversed these negative effects by normalizing the endothelin-1 axis and reducing DNA damage, which contributed to the effects of SG to ameliorate endothelial function and prevent lung cancer.

INTRODUCTION

Emerging evidence implies that obesity is an independent risk factor for multiple types of cancer[1], and type 2 diabetes mellitus (T2DM), an obesity-related concomitant disease, can favor a suitable environment for tumor formation, progression, and metastasis by influencing several biochemical and physiological factors, such as adipokines, inflammatory mediators, and altered microbiome[2]. Endothelial dysfunction (ED) is a complication of both obesity[3] and T2DM[4], which refers to a proinflammatory and prothrombotic state[5], and is capable of impairing blood vessels, causing cardiovascular disease and end-organ damage. Fundamentally speaking, the anomaly of endothelins (ETs) is caused by the disrupted ET axis. ETs are a group of proteins comprising three 21-amino acid peptides (ET-1, ET-2, and ET-3), two distinct rhodopsin-like G protein-coupled receptor subtypes (ET-A and ET-B), and ET-converting enzymes (ECEs), which all jointly facilitate the generation of biologically active ETs[6]. Previous research has indicated that the ET axis effects numerous signaling pathways involved in the mediation of apoptosis and growth in different cells[7]. In cancer cells, the ET axis activates autocrine/paracrine feedback loops, promoting the development and progression of tumors[8], such as lung cancer[9], *via* several different mechanisms[10].

Among the commonly known isoforms of ETs, ET-1 is the most clinically relevant which has the highest expression[11] and makes a significant contribution to ED in many ways[5]. ET-1 is originally secreted by endothelial cells through both constitutive and regulated (or rapid release) pathways[12], of which the downstream effects are regulated by ET-A and ET-B[6]. ET-A is mainly expressed in vascular smooth muscle

cells, while ET-B is expressed in endothelial cells, vascular smooth muscle cells, macrophages, and platelets[13]. Several processes activated by the non-linear signaling network of extracellular binding of ET-1 to ET-A, for instance, cell proliferation, apoptosis, cell invasion and metastasis, angiogenesis, osteogenesis, and nociception[14-16], are involved in normal cell function as well as the development and progression of cancer. Hence, due to an organic abundance in both ET-A and ET-B, ET-1 plays various roles in mediating pulmonary carcinogenesis[17-19], and ED is a predictor of the diagnosis and prognosis of lung cancer[20]. Meanwhile, as a common but sometimes fatal lesion in normal cells, DNA damage can lead to canceration, where the double-strand break is deemed the most harmful type, resulting in the general and instant DNA damage response in cells and the phosphorylation of Ser-139 of the H2A histone family member X (H2AX) at the site of DNA damage (γ-H2AX foci)[21]. Hence, marking nuclear γ-H2AX in a certain cell population is considered a brilliant way of recognizing early DNA damage, which has been frequently applied in cancer studies[22-24].

Bariatric surgeries are universally performed as an effective treatment for severe obesity, T2DM, and other related comorbidities[25]. Besides, whether in clinical trials or animal studies, they have been shown to prevent or lower the risk of cancers[26-29], including lung cancer[30]. Unfortunately, compared to these apparent effects, little is known about the underlying mechanisms of lowered cancer risk after bariatric surgeries. Thus, based on the scarcity of relevant studies and the negative impacts of obesity and T2DM on endothelial function, tumor development, and the essential role of ET-1 axis in tumor pathogenesis of the lung, we speculated that there may be a correlation between the ET-1 axis with ameliorated endothelial function and lowered risk of cancer following bariatric surgeries. Herein, using an obese and diabetic rat model induced with a high-fat diet and streptozotocin, we investigated the potential effect of sleeve gastrectomy (SG) in improving endothelial function and lowering the risk of carcinogenesis by normalizing the ET-1 axis and ameliorating DNA damage.

MATERIALS AND METHODS

Animals and study design

The protocol of the current study is shown in Figure 1. Seventy male Wistar rats (200 g average body weight; SPF Biotechnology Co., Ltd., Beijing, China) were housed in independent ventilated cages under constant ambient temperature (24-26 °C) and humidity (50%-60%) in a 12-h light/dark cycle. The study protocol was approved by the Institutional Animal Care and Use Committee of The First Affiliated Hospital of Shandong First Medical University (China), and every effort was made to minimize the pain and discomfort of the study subjects. And in accordance with the 3R principle of humane experimental technique[31] to minimize the number of animals used, five animals were included in each sub-group that was divided by the postoperative time points (every 4 wk, see below), and to meet this sample size, animals were unequally and randomly divided into the following three groups based on their differences in postoperative mortality estimated during preliminary experiment (data not shown).

Group 1 representing control (C; *n* = 15): Animals were given a standard diet (15% of calories as fat; Laboratory Animal Center of Shandong University, Shandong, China) during the whole protocol, with no intervention made.

Group 2 representing sham-operated control (SH; *n* = 22): Animals were fed a high-fat diet (40% fat, 42% carbohydrate, and 18% protein, as a total percentage of calories; Xietong Pharmaceutical Bio-engineering Co., Ltd., Jiangsu, China) for 8 wk and then received intraperitoneal injection of streptozotocin at a dose of 30 mg/kg body weight (0.01 mol/L citrate buffer, pH 4.5; Sigma-Aldrich, St. Louis, MO, United States) to induce hyperglycemia, followed by a sham surgery 1 wk later. In this group, two rats were excluded due to unaltered blood glucose after injection [fasting blood glucose (FBG) < 11.1 mmol/L for 3 d in a row]. Ultimately, 20 rats were qualified for further processing.

Group 3 representing SG-operated (*n* = 33): T2DM was induced exactly the same as the SH group, followed by SG at 1 wk after injection. For this group, three rats were excluded according to the same criteria as above.

Surgical procedures

Operations were performed following overnight fasting, with anesthesia being achieved by applying gaseous anesthesia (2% isoflurane). SG was performed as previously described[32]. Briefly, it involved the following steps: (1) A 4-cm midline epigastric incision was made to identify the structures; (2) The gastric omentum was

Figure 1 Flow chart of the study protocol. ELISA: Enzyme-linked immunosorbent assay; FBG: Fasting blood glucose; OGTT: Oral glucose tolerance test; PCR: Polymerase chain reaction; SG: Sleeve gastrectomy; STZ: Streptozotocin; WB: Western blot; γ-H2AX foci: H2A histone family member X focus assay.

dissected and the gastric cardium was disclosed; (3) The short gastric vessels, related gastroepiploic vessels, and branches of the left gastric vessels in the greater curvature were ligated and transected using 7-0 silk suture (Ningbo Cheng-He Microsurgical Instruments Factory, Zhejiang, China); (4) The gastric fundus and a large portion of the gastric body were removed; and (5) The residual stomach was closed using 5-0 silk suture (Ningbo Cheng-He Microsurgical Instruments Factory).

Laparotomy was performed on the SH rats to expose the stomach, esophagus, and small intestine. No other intervention was made. Furthermore, operative time was prolonged to induce a degree of comparable anesthetic stress that experienced by the SG rats.

For postoperative care, mixed tap water (4 g of white granulated sugar, 0.25 g of cefuroxime, and 0.4 g of ibuprofen dissolved in 500 mL of tap water) was given to rats in the SH and SG groups at 24 h after the operation for 3 d. Then, approximately 7 g of Total Nutrition Formula for Dietary Fiber (Nutren Fibre; Nestlé Health Science, Epalinges, Switzerland) was dissolved in 500 mL tap water and given for another 3 d. From postoperative day 7, all operated animals were given free access to a standard diet and tap water until the end of the protocol, same as the C group as abovementioned.

All C rats survived until the end of the protocol. Two rats in the SH group died of hyperglycemia during the postoperative period of 3 mo. Eighteen rats in the SG group survived, while the other 12 died of the following causes: Gastric leakage (n = 3), infection (n = 3), intestinal obstruction (n = 4), and unknown cause (n = 2; inconclusive on autopsy).

In all, 15, 18, and 18 rats survived in the C, SH, and SG groups, respectively, and to favor an equal sample size for each group, five rats in each group were randomly euthanatized by applying an overdose of 10% chloral hydrate (5 mL/kg) every 4 wk after operation. Hence, 15 rats of each group were included in this study. Body weight and food intake were monitored before the surgery and weekly in the first 2 wk after surgery, and then once in every 2 wk until the end of the protocol at the 12th week after the operation. Blood samples were collected before the surgery and mensal euthanasia, followed by tissue sampling and preparation for further testing.

Blood chemistry

FBG level was measured with a glucometer (Roche OneTouch Ultra®; LifeScan, Johnson and Johnson, Milpitas, CA, United States) at the abovementioned time intervals, same as measurements of body weight and food intake. Blood was collected from the tail vein in unconscious rats and samples were centrifuged at 3000 rpm for 8 min; the serum was then extracted and stored at -80 °C. Serum insulin was measured with ELISA kits (CUSABIO, Hubei Province, China). Furthermore, the homeostasis model assessment of insulin resistance (Homa-IR) was used to estimate the degree of insulin resistance, which was calculated with the following formula: Homa-IR = fasting serum insulin (mIU/L) × FBG (mmol/L)/22.5[33].

Oral glucose tolerance test

Oral glucose tolerance test (OGTT) was performed before the operations and at 4, 8, and 12 wk after surgery. After an overnight fast, rats were administered with 1 g/kg glucose by oral gavage. Blood glucose was measured in conscious rats at 0, 10, 30, 60, and 120 min after the gavage. Area under the curve for OGTT was calculated by the trapezoidal method.

Quantitative real-time polymerase chain reaction

Total RNA was extracted using TRIzol reagent (Invitrogen, Carlsbad, CA, United States). The cDNA was synthesized using random primers (Servicebio, Hubei, China) and Revert Aid First Strand cDNA Synthesis Kit (#K1622; Thermo Fisher Scientific, Waltham, MA, United States). Quantitative real-time polymerase chain reaction (PCR) was performed on a Cycler System (StepOne Plus; Applied Biosystems Inc., Foster City, CA, United States), with the analyses being performed using the FastStart Universal SYBR Green Master (Servicebio) in a total PCR reaction containing 25 µL of quantitative PCR Mix, 2.0 µL of 7.5 µmol/L primers, 2.5 µL of reverse transcription product, and 8.0 µL of double-distilled H_2O. The specific sequences of the primers for analyzed genes are shown in Table 1.

Western blot analysis

Lung tissues were homogenized and centrifuged at 12000 rpm for 10 min. Supernatants were extracted and the protein concentration was determined with a BCA kit (G2026; Servicebio). Protein solution was added into the loading buffer (G2013; Servicebio) in a ratio of 4:1 and denatured in boiling water for 15 min. Samples were loaded on 5% SDS-PAGE gels (Servicebio), then separated by

Table 1 Specific sequences of primers used in polymerase chain reaction analysis

Gene	Primer sequence, 5'-3'	GenBank No.	Length, bp	Annealing temperature, °C
GAPDH	F: CTGGAGAAACCTGCCAAGTATG	NM_017008.4	138	60
	R: GGTGGAAGAATGGGAGTTGCT			
ET-1	F: TCTGCCACCTGGACATCATCTG	NM_012548.2	205	60
	R: CTTTGGGCTCGGAGTTCTTTGT			
ET-A	F: ACCGCCATTGAAATTGTCTCC	NM_012550.2	173	60
	R: AGCCACCAGTCCTTCACGTCTT			
ET-B	F: CCAAAGACTGGTGGCTGTTCA	XM_006252431.3	183	60
	R: CAAACACGAGGACCAGGCAG			
ECE-1	F: CACAACCAAGCCATCATTAAGC	NM_053596.2	275	60
	R: TTGGAGTCGGCACTGACATAGA			

F: Forward; R: Reverse.

electrophoresis and transferred onto polyvinylidene fluoride membranes (Millipore, Burlington, MA, United States). After being blocked in 5% fat-free milk for 1 h, membranes were incubated overnight with the following primary antibodies: ET-1 (ab117757; Abcam, Cambridge, United Kingdom), ET-A (ab85163; Abcam), ET-B (ab262694; Abcam), ECE-1 (sc-376017; Santa Cruz Biotechnology, Dallas, TX, United States), and GAPDH (ab9485; Abcam). The next day, the membranes were incubated in horseradish peroxidase-conjugated secondary antibodies, which were diluted 3000 times with Tris-buffered saline Tween-20. Bands were visualized with ECL solution (Servicebio) and the band intensity was quantified using ImageJ software (National Institutes of Health, Bethesda, MA, United States).

Immunohistochemical analysis of γ-H2AX

Paraffin sections (5 μm) of the lungs were deparaffinized, rehydrated in a solution series (xylene 15 min thrice, absolute ethyl alcohol 5 min twice, 85% ethanol 5 min once, and 75% ethanol 5 min once), and washed with distilled water. Then, they were put into citrate antigen retrieval solution (pH 6.0), followed by a 3% hydrogen peroxide solution and incubation in darkness at room temperature for 25 min. Afterwards, the slides were placed in phosphate-buffered saline (pH 7.4) and washed thrice on the decolorization shaker (5 min each) to block the endogenous peroxidase activity after deparaffinization and antigen retrieval. Anti-histone γ-H2AX antibody (ChIP grade, 1:2000, ab20669; Abcam) was used and an appropriate elite horseradish peroxidase-diaminobenzidine system was applied to reveal antibody. The sections were counterstained with hematoxylin. Finally, the sections were dehydrated through an alcohol and xylene gradient and sealed with neutral gum.

When completed, the sections were made into electronic slides using the Pannoramic Digital Slide Scanners (Pannoramic DESK, P-MIDI, P250 and P1000; 3DHISTECH Ltd., Budapest, Hungary). Then, a slide representing each animal was randomly selected and covered with FOV rectangles in CaseViewer v2.0 (3DHISTECH Ltd.), and five fields at× 800 magnification from different rectangles were chosen for subsequent image analysis using the ImageJ software for semi-quantitative analysis. A γ-H2AX-positive nucleus (*i.e.*, a double-strand break-damaged nucleus within a cell population counterstained by hematoxylin) was easily distinguishable when a homogeneous brown precipitate was observed covering partial or entire nucleus compared to the undamaged nucleus, which was colored blue. Levels of DNA damage in each group at different time points are expressed as the average percentage of γ-H2AX positive (brown-stained) to negative (blue-stained) nuclei of the sections.

Statistical analysis

Results were analyzed using two-way ANOVA with Tukey's multiple comparison tests (GraphPad Prism 8.3; GraphPad, La Jolla, CA, United States). P values < 0.05 were considered significant. Data are expressed as the mean ± SE of the mean.

RESULTS

Metabolic parameters

SG brought a significant improvement to the metabolic disorder (Figure 2). An increase in both body weight and food intake was noted in all the three groups, where C rats had a steady increase but the other two groups (SH and SG) showed a decline during the early postoperative stage (Figure 2A and B, Tables 2 and 3). In terms of the glycemic change (Figure 2C-F, Tables 4-7), the FBG of the C group stayed nearly unaltered, which was verified by OGTT, with a slight increase being noted. Similarly, despite the elevation in the fasting serum insulin level, the Homa-IR of the C animals did not change much, either. The SH group, in contrast, showed a continual FBG increase, which was further reflected by OGTT. Moreover, although the fasting insulin levels of the C group were not significantly different from those of the other two groups at most of the time points, the SH animals demonstrated an aggravated insulin resistance. On the other hand, the rapid reduction in body weight and in food intake was accompanied by the FBG returning to normal in the SG rats; the results of OGTT were nearly the same as in C rats. However, from the middle and late postoperative periods, the FBG of some SG rats began to rise. The fasting serum insulin levels of the SG animals increased after surgery but were not significantly different from those of the other groups. Nevertheless, similar to the results of FBG and OGTT, Homa-IR of the SG rats increased with age but was still much lower than that of the SH group. These results indicated that SG improved glycometabolism and insulin sensitivity in obese and diabetic rats with a rapid weight loss and reduction in food intake.

Gene expression of ET-1 axis

The mRNA expression of genes of the ET-1 axis are shown in Figure 3 and Tables 8-11. On the whole, C rats manifested steady expression in these genes, where an increase was notable in SH animals, even though the differences between the other two groups were not so conspicuous throughout the postoperative period. SG showed an effect of lowering, in other words, normalizing, the overexpressed genes. For *ET-1*, the SG group had lower expression than the C group at postoperative weeks 4 and 8, which was significantly lower than that in SH rats at the 8th and 12th wk after surgery. For *ET-A*, both SH and SG animals had an elevation at the last time point, yet a significant difference existed only between the C and SH animals. Similarly, with an obvious rise in *ET-B* expression at postoperative week 12, the SH group had significantly higher expression than the other two. As for *ECE-1*, an elevation was seen in both the SH and SG groups over time, with the former being significantly higher than the latter at the first time point. The C group was opposite, having much lower expression than the SH group at postoperative weeks 4 and 12. Although not entirely capable of offsetting the gap between C and SH animals at all time intervals, the SG group had normalized abnormalities in the ET-1 axis, indeed.

Protein expression of ET-1 axis

Results of protein expression of the ET-1 axis were not absolutely consistent with those from PCR tests (Figure 4 and Tables 12-15). In terms of the expression of both ET-1 and ET-A, a decrease was seen in the C group, which was opposite in the SG group. The SH group, however, was inconstant in the expression of ET-1 and the same as that in the SG group for ET-A. For both ET-1 and ET-A, the C group had lower expression, which was directionally opposite in the SG group; the SH group, however, was inconstant for the former but the same as in the SG group for the latter. The C group showed nearly steady or slightly increased expression in ET-B and ECE-1 as the animals aged, and the SG group showed gradually decreasing expression in these two proteins. The SH group showed continually increasing expression in ET-B and a maintained high level of ECE-1 expression.

DNA damage

The representative images of the γ-H2AX assay are shown in Figure 5. These images provide an intuitionistic comparison among groups, where it can be seen that there were more γ-H2AX-positive nuclei (red arrows) in the SH group than in the other two groups (Figure 5A). Furthermore, the semi-quantification analysis confirmed that the SH rats had more γ-H2AX-positive nuclei compared to the other two groups (Figure 5B and Table 16), indicating that cells in obese and diabetic rat lungs suffer from much more severe DNA damage than those in healthy and SG-operated rats.

DISCUSSION

Our rat model-based study demonstrated elevated expression of genes and proteins of the ET-1 axis and increased DNA damage in obese and diabetic lungs, indicating a deteriorated endothelial function and a greater risk of cancer development. However,

Table 2 Comparisons of body weight (g) among groups

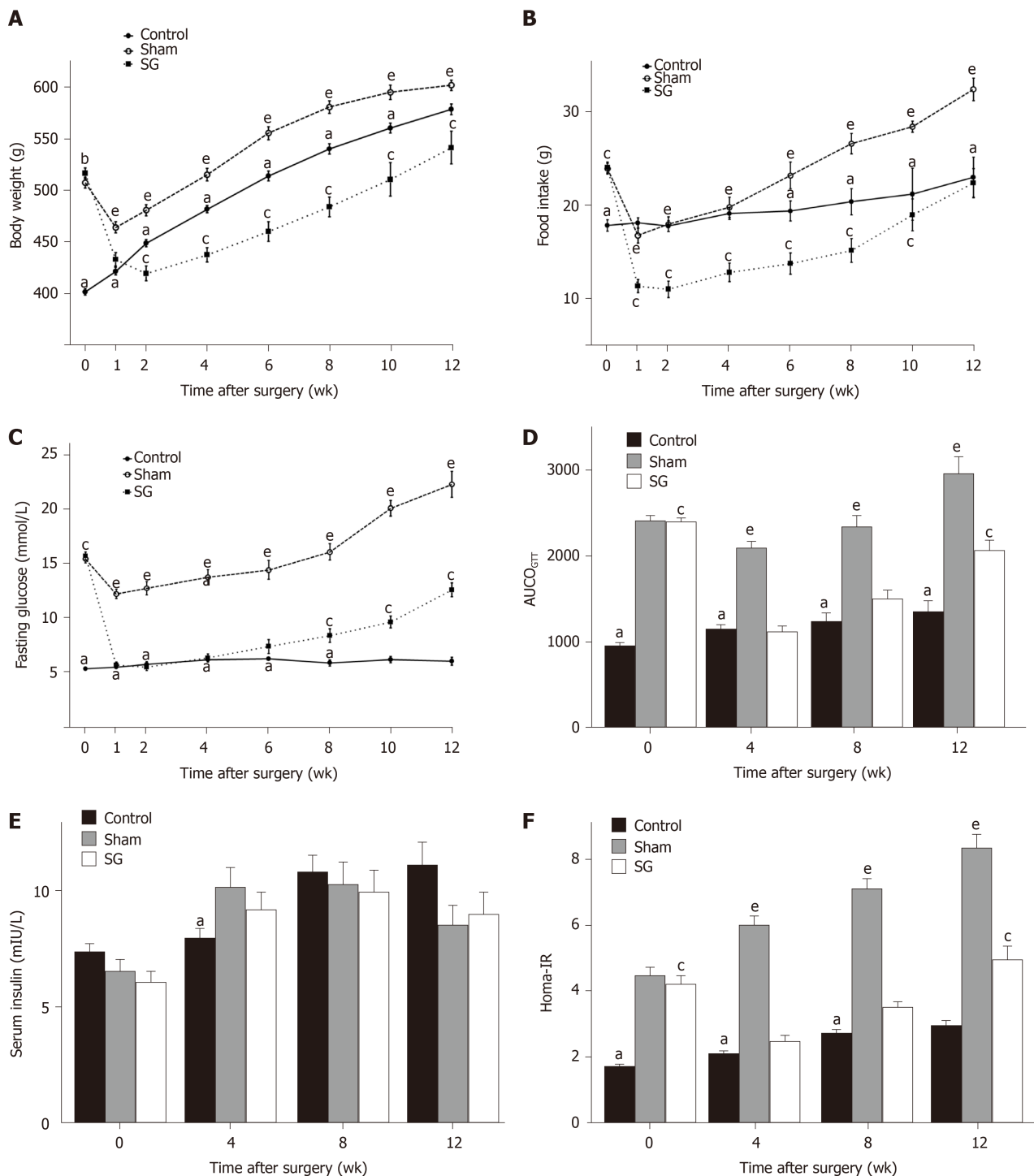| Time after surgery (wk)	C	SH	SG	P value		
				C *vs* SH	C *vs* SG	SH *vs* SG
0	401.7 ± 13.0	507.5 ± 20.4	516.6 ± 20.1	< 0.0001	< 0.0001	0.4768
1	421.5 ± 13.9	464.1 ± 21.0	433.0 ± 25.6	< 0.0001	0.3071	0.0003
2	448.8 ± 13.0	480.8 ± 21.6	419.5 ± 27.6	0.0002	0.0006	< 0.0001
4	481.7 ± 13.9	515.3 ± 23.1	437.5 ± 27.0	< 0.0001	< 0.0001	< 0.0001
6	513.8 ± 14.8	555.5 ± 19.9	460.1 ± 30.2	< 0.0001	< 0.0001	< 0.0001
8	540.2 ± 16.1	580.9 ± 19.1	484.1 ± 30.2	< 0.0001	< 0.0001	< 0.0001
10	560.4 ± 10.6	595.2 ± 15.4	510.6 ± 36.5	0.0284	0.0008	< 0.0001
12	578.6 ± 12.1	602.0 ± 11.2	541.4 ± 35.4	0.1953	0.0174	< 0.0001

Data are expressed as the mean ± SD. C: Control; SH: Sham; SG: Sleeve gastrectomy.

all these alterations were able to be ameliorated by SG, a marvelous treatment for metabolic disorder that is competent in preventing or lowering the risk of various types of cancer as well.

Being crucial for maintaining vascular homeostasis, the endothelium modulates blood flow, nutrient delivery, vascular smooth muscle cell proliferation and migration, fibrinolysis, coagulation, inflammation, and platelet and leukocyte adherence[34]. In contrast, ED, a common complication of both obesity and T2DM, is one of the concrete manifestations of this homeostasis being destroyed, which ultimately results in hypertension, thrombosis, and various cardiovascular diseases[35]. So far, it has been known that adipose tissue inflammation, nitric oxide bioavailability, insulin resistance, and oxidized low-density lipoprotein are the main contributors to obesity-related ED[35]. Under the diabetic condition, ED is mainly caused by hyperglycemia, insulin resistance, abnormal cell growth factors, and vasoactive substances[36]. With its elevated release from adipose tissue, ET-1 exerts an anti-insulin effect by reducing the expression of insulin receptor, insulin receptor substrate-1, and phosphodiesterase-3B, while increasing the expression of ET-B[37]. As a result, more fat deposition is induced by fatty acids released from the visceral adipose tissue because of the insulin resistance[38]. Combined with the dramatically increased protein expression of ET-A, ET-1 leads to more lipolysis *via* the activation of ET-A in adipose tissue[35]. On the other hand, the balance between endothelial-derived relaxation and contraction factors is disrupted in T2DM where the vasodilator factors (*i.e.*, nitric oxide, prostacyclin, and endothelial-derived hyperpolarizing factor) and vasoconstricting factors (*i.e.*, ET-1, angiotensin II, and prostaglandin) are inordinate[36]. ET-1, as one of the serum markers of ED, can be transcriptionally increased by enhanced glycosylated end-products (known commonly as AGEs) in patients with poorly controlled blood glucose[39]. Therefore, ET-1 is considered a predictive factor for diabetic complications[40].

Regarding the close relation of the ET axis with cancer development, former studies have stated that cancers can be divided into three types based upon the expression level of endothelin receptors[41], and lung cancer belongs to the third type based upon its characteristic overexpression of ET-1, ET-A, and ET-B altogether[42], which is in line with our findings. The overexpression of ET-A in cancer has been shown to be associated with invasive biological behavior[43], while the expression of ET-B has been linked to lymphoid infiltration[44]. Considering the important role of the ET-1 axis in carcinogenesis, it has been targeted in pharmacotherapy for cancers, such as ECE inhibition and antagonism of ET-A and ET-B[45]. Although a noncancerous animal model was used, and the similar ET-1 alteration profile may not lead to cancer in these obese and diabetic animals, it is still a perfect example of obesity and T2DM providing a suitable environment for tumor formation. Further comparisons between the SH and SG groups of rats suggested that SG normalized the ET-1 activity profoundly, just as it did in reducing body weight and stabilizing glycometabolism. Consistent with this, it was reported in a clinical trial that SG can reduce plasma ET-1 levels[46]. Moreover, it was suggested by another study, which made a comparison to normalized blood glucose, that weight loss is much more important in the regulation of circulating levels of ET-1 in morbidly obese subjects[47], which also explains why the T2DM in some SG animals seemed to relapse in the middle and late periods after surgery while they still showed positive changes in the ET-1 axis.

DNA damage is a parameter of evaluating the risk of developing cancer, and it

Figure 2 Comparisons of metabolic parameters among groups. A: Body weight; B: Food intake; C: Fasting glucose level; D: Area under the curve of oral glucose tolerance test; E: Fasting serum insulin level; F: Homeostasis model assessment of insulin resistance compared to sham-operated and control rats. [a]$P < 0.05$: Control *vs* sham; [c]$P < 0.05$: Control *vs* sleeve gastrectomy; [e]$P < 0.05$: Sham *vs* sleeve gastrectomy. AUC_{OGTT}: Area under the curve of oral glucose tolerance test; Homa-IR: Homeostasis model assessment of insulin resistance; SG: Sleeve gastrectomy.

affects DNA replication, leading to mutations, and lowers cell metabolism and survival[48]. In obesity, DNA damage is closely related to chronic inflammation, reactive oxygen species, oxidative stress, and cytokines[49]. Meanwhile, the activation of certain oncogenes induced by DNA damage can cause diabetes[50,51]. And as introduced, diabetes is correlated with DNA damage, mutation, and canceration[52]. Since γ-H2AX is a regular marker of DNA damage response, its level can reflect the risk of canceration. A higher level of γ-H2AX was found in precancerous tissues, when compared to that in tumors in a lung cancer rat model induced by chronic inflammation[53]. Likewise, high level γ-H2AX is also related to oxidative stress and type 1 DM in adolescents[54]. While obesity and diabetes injure the lungs by causing

Table 3 Comparisons of food intake (g/d) among groups

Time after surgery (wk)	C	SH	SG	P value		
				C *vs* SH	C *vs* SG	SH *vs* SG
0	17.9 ± 2.4	23.9 ± 2.2	24.1 ± 2.2	< 0.0001	< 0.0001	0.9932
1	18.1 ± 2.2	16.8 ± 3.2	11.4 ± 2.7	0.5071	< 0.0001	< 0.0001
2	17.8 ± 2.4	18.0 ± 3.1	11.1 ± 3.4	0.9848	< 0.0001	< 0.0001
4	19.1 ± 2.4	19.8 ± 4.1	12.9 ± 3.8	0.8433	< 0.0001	< 0.0001
6	19.4 ± 3.4	23.2 ± 4.5	13.8 ± 3.6	0.0274	0.0005	< 0.0001
8	20.4 ± 4.5	26.6 ± 3.5	15.2 ± 4.0	< 0.0001	0.0014	< 0.0001
10	21.2 ± 6.2	28.4 ± 1.3	19.0 ± 3.8	0.0018	0.5398	< 0.0001
12	23.0 ± 4.8	32.4 ± 2.7	22.4 ± 3.4	< 0.0001	0.9550	< 0.0001

C: Control; SH: Sham; SG: Sleeve gastrectomy.

DNA lesions in nuclei as previously described[55,56], the SG rats in our study presented much more cells with a normal morphology. In line, recent studies have found that bariatric surgeries are effective in reducing DNA damage indeed, in both humans[57,58] and animals[59]. Based on the possible mechanism of the DNA damage caused by obesity and diabetes, we can assume that SG exhibited a positive role in preventing cancer by eliminating the harmful factors that contribute to the genetic damage.

In summary, obesity and T2DM significantly increase the risk of multiple diseases and cancer, in which, disruption in the ET-1 axis leads to ED and an increased risk of developing lung cancer. Nevertheless, with a profound effect of reducing body weight and improving glycometabolism and insulin sensitivity, SG improves endothelial function and exerts a protective role in preventing lung cancer by normalizing the ET-1 axis and weakening the effects of DNA damage. In the context of the current scarcity of basic research covering both cancer and bariatric surgeries, an attempt was made in the current study to provide new perspectives and lines of evidence for the role of SG in preventing cancer. We believe that these findings will deepen our understanding of anticancer effects of bariatric surgeries and broaden the theoretical basis for the evaluation of the surgical effect of SG, especially in supporting the clinical findings of bariatric surgery for lowering the risk of lung cancer. However, more future studies are warranted to uncover the other potential mechanisms of such effects.

Table 4 Comparisons of fasting blood glucose (mmol/L) among groups

Time after surgery (wk)	C	SH	SG	P value		
				C *vs* SH	C *vs* SG	SH *vs* SG
0	5.3 ± 0.7	15.4 ± 1.5	15.7 ± 1.3	< 0.0001	< 0.0001	0.8776
1	5.5 ± 0.7	12.2 ± 1.6	5.7 ± 1.1	< 0.0001	0.9423	< 0.0001
2	5.7 ± 1.0	12.7 ± 2.3	5.5 ± 1.2	< 0.0001	0.8982	< 0.0001
4	6.2 ± 1.0	13.8 ± 2.7	6.3 ± 1.4	< 0.0001	0.9534	< 0.0001
6	6.3 ± 0.6	14.4 ± 2.7	7.4 ± 2.0	< 0.0001	0.2619	< 0.0001
8	5.9 ± 0.9	16.1 ± 2.4	8.4 ± 1.9	< 0.0001	0.0017	< 0.0001
10	6.2 ± 0.7	20.1 ± 1.6	9.6 ± 1.3	< 0.0001	0.0023	< 0.0001
12	6.0 ± 0.8	22.3 ± 2.7	12.6 ± 1.5	< 0.0001	< 0.0001	< 0.0001

C: Control; SH: Sham; SG: Sleeve gastrectomy.

Table 5 Comparisons of areas under curve of oral glucose tolerance test among groups

Time after surgery (wk)	C	SH	SG	P value		
				C *vs* SH	C *vs* SG	SH *vs* SG
0	956 ± 123	2419 ± 197	2407 ± 147	< 0.0001	< 0.0001	0.9907
4	1148 ± 214	2101 ± 293	1125 ± 226	< 0.0001	0.9651	< 0.0001
8	1241 ± 316	2346 ± 408	1507 ± 314	< 0.0001	0.0591	< 0.0001
12	1353 ± 282	2967 ± 421	2075 ± 247	< 0.0001	< 0.0001	< 0.0001

C: Control; SH: Sham; SG: Sleeve gastrectomy.

Table 6 Comparisons of fasting serum insulin levels (mIU/L) among groups

Time after surgery (wk)	C	SH	SG	P value		
				C *vs* SH	C *vs* SG	SH *vs* SG
0	7.385 ± 1.359	8.243 ± 2.349	6.104 ± 1.734	0.6134	0.2858	0.8341
4	7.989 ± 1.542	8.238 ± 1.597	9.212 ± 2.835	0.0263	0.3189	0.4710
8	10.808 ± 2.309	10.348 ± 1.898	9.946 ± 3.054	0.8770	0.6826	0.9362
12	11.146 ± 2.173	7.734 ± 1.525	9.042 ± 2.005	0.1864	0.3240	0.9439

C: Control; SH: Sham; SG: Sleeve gastrectomy.

Table 7 Comparisons of insulin resistance (mIU × mmol/L^2) among groups

Time after surgery (wk)	C	SH	SG	P value		
				C *vs* SH	C *vs* SG	SH *vs* SG
0	1.721 ± 0.157	4.474 ± 1.078	4.216 ± 1.061	< 0.0001	< 0.0001	0.6563
4	2.136 ± 0.234	5.988 ± 1.227	2.503 ± 0.667	< 0.0001	0.4289	< 0.0001
8	2.744 ± 0.309	7.116 ± 0.934	3.525 ± 0.656	< 0.0001	0.0811	< 0.0001
12	2.944 ± 0.365	8.341 ± 0.941	4.979 ± 0.833	< 0.0001	0.0003	< 0.0001

C: Control; SH: Sham; SG: Sleeve gastrectomy.

Table 8 Comparisons of endothelin-1 mRNA expression among groups

Time after surgery (wk)	C	SH	SG	*P* value		
				C *vs* SH	C *vs* SG	SH *vs* SG
4	1.51 ± 1.21	2.33 ± 1.08	1.31 ± 0.39	0.3293	0.9316	0.1828
8	1.11 ± 0.41	2.88 ± 0.80	0.87 ± 0.39	0.0100	0.9085	0.0033
12	1.56 ± 0.86	3.07 ± 1.55	1.65 ± 0.63	0.0318	0.9878	0.0449

C: Control; SH: Sham; SG: Sleeve gastrectomy.

Table 9 Comparisons of endothelin receptor A mRNA expression among groups

Time after surgery (wk)	C	SH	SG	*P* value		
				C *vs* SH	C *vs* SG	SH *vs* SG
4	1.17 ± 0.77	1.77 ± 0.88	1.09 ± 0.59	0.4552	0.9859	0.3669
8	1.57 ± 0.42	1.73 ± 0.55	1.21 ± 0.62	0.9460	0.7454	0.5501
12	1.61 ± 0.97	2.92 ± 1.03	2.71 ± 1.01	0.0334	0.0859	0.9047

C: Control; SH: Sham; SG: Sleeve gastrectomy.

Table 10 Comparisons of endothelin receptor B mRNA expression among groups

Time after surgery (wk)	C	SH	SG	*P* value		
				C *vs* SH	C *vs* SG	SH *vs* SG
4	1.06 ± 0.40	0.96 ± 0.27	0.94 ± 0.58	0.9581	0.9393	0.9981
8	0.98 ± 0.65	1.45 ± 0.62	1.07 ± 0.68	0.3994	0.9666	0.5442
12	1.00 ± 0.53	2.08 ± 0.84	1.17 ± 0.37	0.0141	0.8937	0.0419

C: Control; SH: Sham; SG: Sleeve gastrectomy.

Table 11 Comparisons of endothelin-converting enzyme-1 mRNA expression among groups

Time after surgery (wk)	C	SH	SG	*P* value		
				C *vs* SH	C *vs* SG	SH *vs* SG
4	1.11 ± 0.61	2.24 ± 0.55	0.99 ± 0.39	0.0191	0.9534	0.0090
8	1.40 ± 0.21	2.35 ± 1.00	1.52 ± 0.57	0.0550	0.9526	0.1031
12	1.32 ± 0.81	2.60 ± 0.73	1.65 ± 0.35	0.0073	0.6881	0.0552

C: Control; SH: Sham; SG: Sleeve gastrectomy.

Table 12 Comparisons of relative endothelin-1 protein expression among groups

Time after surgery (wk)	C	SH	SG	*P* value		
				C *vs* SH	C *vs* SG	SH *vs* SG
4	0.95 ± 0.11	1.10 ± 0.14	0.69 ± 0.10	0.3229	0.0354	0.0007
8	0.68 ± 0.10	1.79 ± 0.25	1.02 ± 0.12	< 0.0001	0.0056	< 0.0001
12	0.60 ± 0.06	1.64 ± 0.20	1.36 ± 0.24	< 0.0001	< 0.0001	0.0229

C: Control; SH: Sham; SG: Sleeve gastrectomy.

Table 13 Comparisons of relative endothelin receptor A protein expression among groups

Time after surgery (wk)				*P* value		
	C	SH	SG	C *vs* SH	C *vs* SG	SH *vs* SG
4	0.87 ± 0.17	0.82 ± 0.13	0.61 ± 0.08	0.7836	0.0036	0.0207
8	0.72 ± 0.16	0.97 ± 0.13	0.82 ± 0.08	0.006	0.44	0.1108
12	0.50 ± 0.09	1.17 ± 0.11	1.03 ± 0.09	< 0.0001	< 0.0001	0.1867

C: Control; SH: Sham; SG: Sleeve gastrectomy.

Table 14 Comparisons of relative endothelin receptor B protein expression among groups

Time after surgery (wk)				*P* value		
	C	SH	SG	C *vs* SH	C *vs* SG	SH *vs* SG
4	1.06 ± 0.11	1.29 ± 0.16	1.26 ± 0.20	0.0575	0.095	0.9697
8	0.54 ± 0.11	1.71 ± 0.16	1.03 ± 0.14	< 0.0001	< 0.0001	< 0.0001
12	1.14 ± 0.08	2.28 ± 0.19	1.00 ± 0.16	< 0.0001	0.2966	< 0.0001

C: Control; SH: Sham; SG: Sleeve gastrectomy.

Table 15 Comparisons of relative endothelin-converting enzyme-1 protein expression among groups
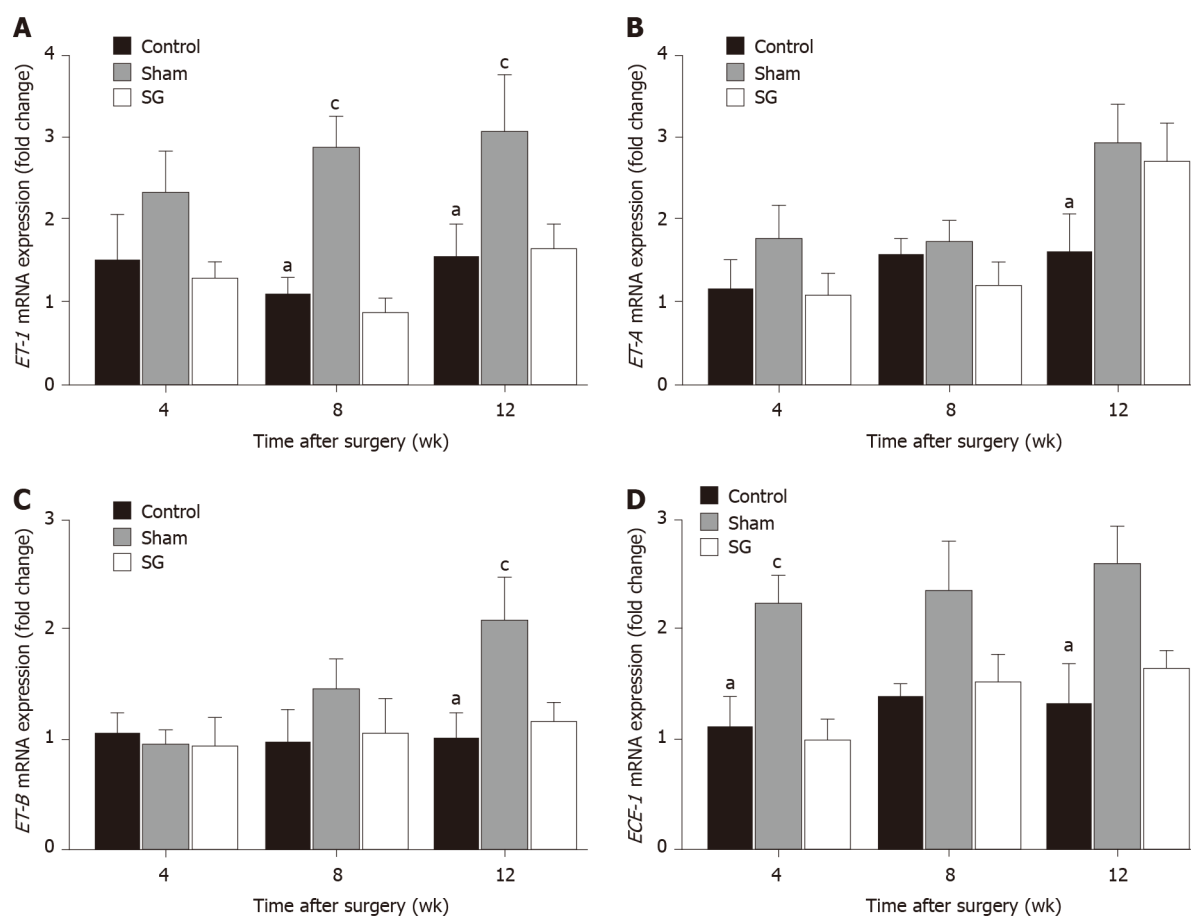
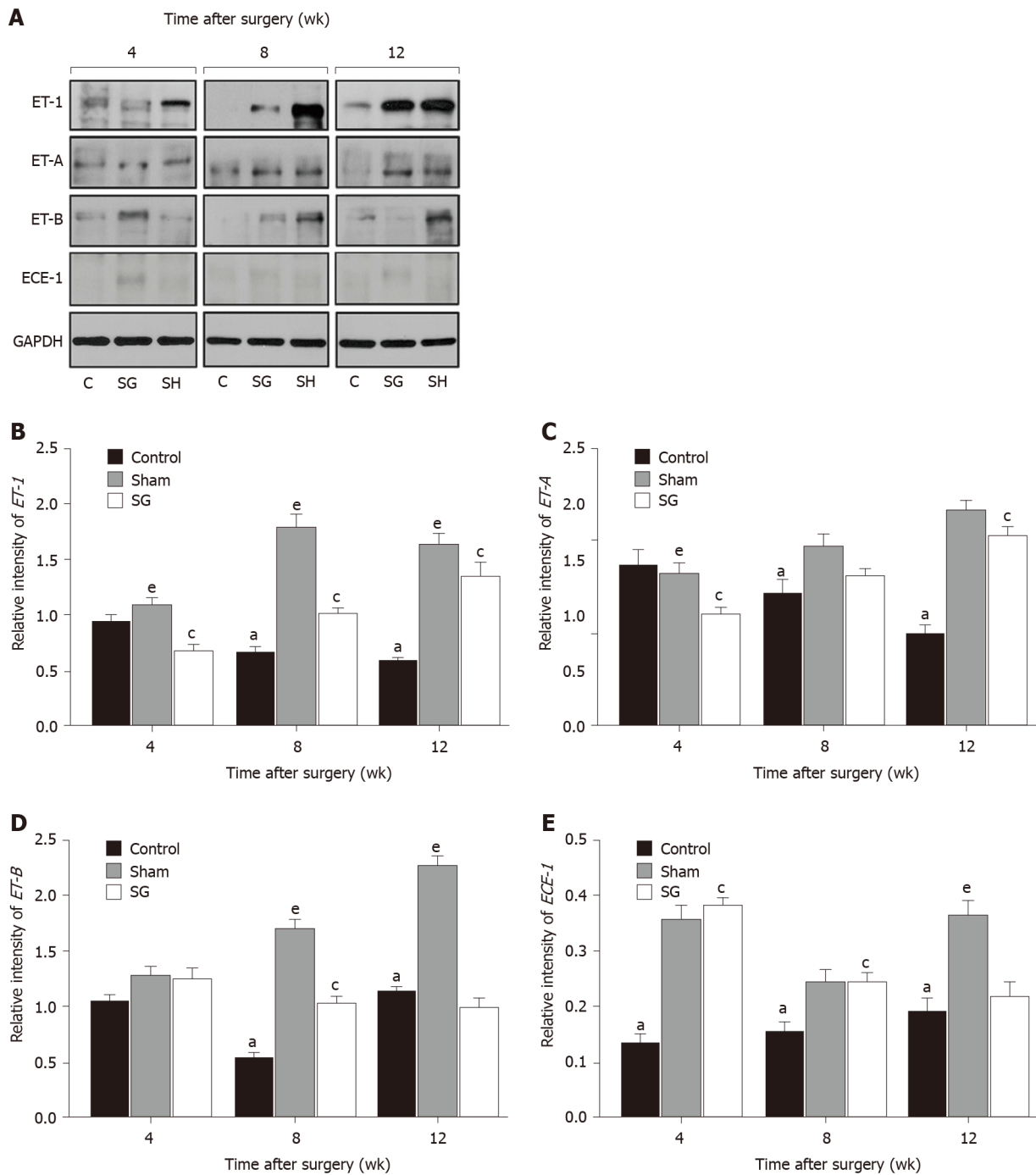| Time after surgery (wk)				*P* value		
	C	SH	SG	C *vs* SH	C *vs* SG	SH *vs* SG
4	0.13 ± 0.03	0.36 ± 0.06	0.39 ± 0.02	< 0.0001	< 0.0001	0.5966
8	0.15 ± 0.04	0.25 ± 0.05	0.24 ± 0.04	0.0123	0.0125	> 0.9999
12	0.19 ± 0.05	0.37 ± 0.06	0.22 ± 0.06	< 0.0001	0.6298	< 0.0001

C: Control; SH: Sham; SG: Sleeve gastrectomy.

Table 16 Comparisons of semi-quantified DNA damage levels (percentage of γ-H2AX-positive cells) among groups

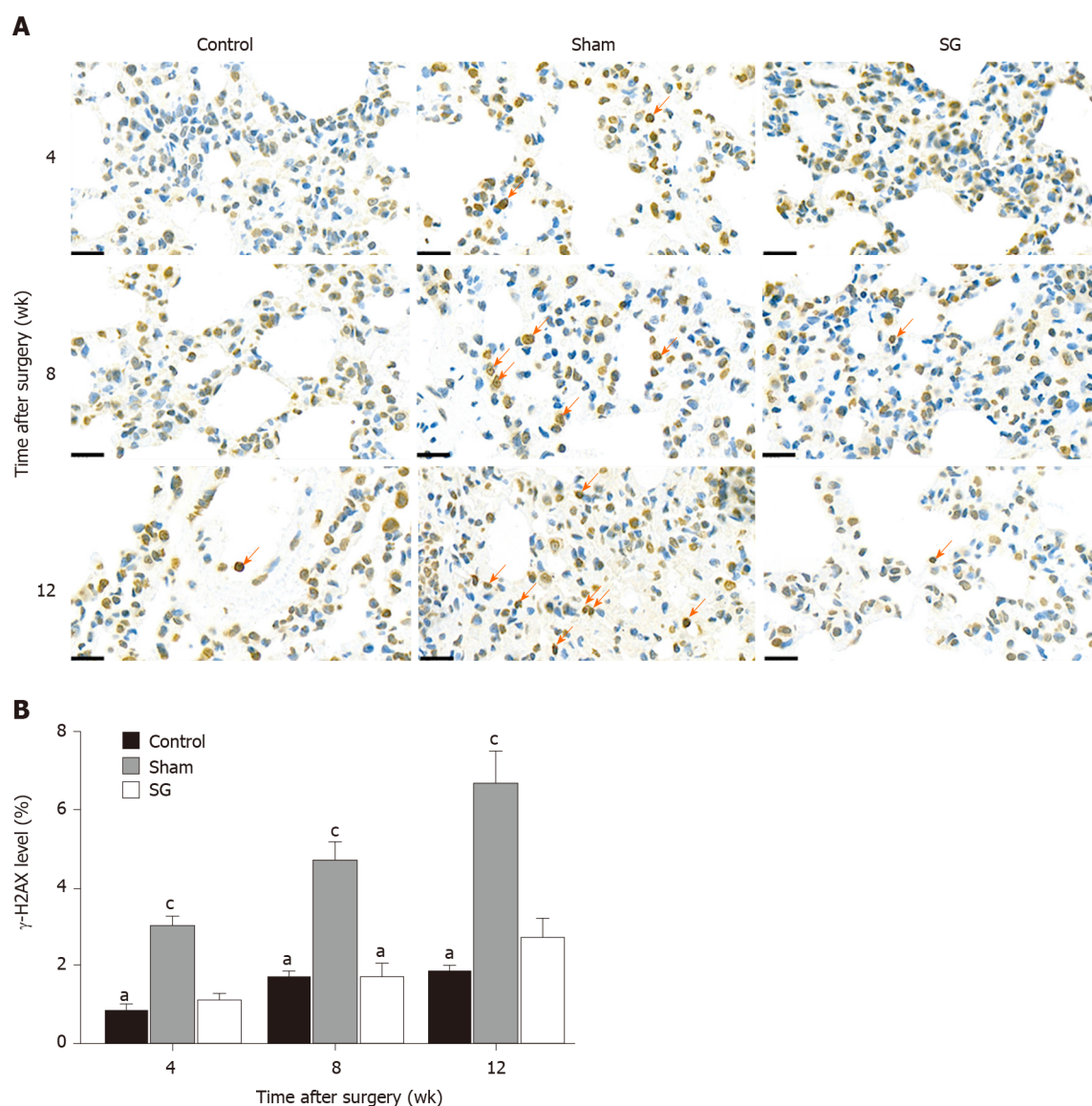| Time after surgery (wk)				*P* value		
	C	SH	SG	C *vs* SH	C *vs* SG	SH *vs* SG
4	0.83 ± 0.43	3.06 ± 0.47	1.15 ± 0.31	0.0009	0.835	0.0046
8	1.71 ± 0.63	4.73 ± 1.04	1.73 ± 0.72	< 0.0001	0.999	< 0.0001
12	1.86 ± 0.37	6.70 ± 1.80	2.75 ± 1.09	< 0.0001	0.2672	< 0.0001

C: Control; SH: Sham; SG: Sleeve gastrectomy.

Figure 3 Expression of genes of the endothelin-1 axis. [a]*P* < 0.05: Control *vs* sham; [c]*P* < 0.05: Sham *vs* sleeve gastrectomy. SG: Sleeve gastrectomy.

Figure 4 Protein expression of the endothelin-1 axis. A: Immunoblotting of the proteins; B-E: Relative band intensity. [a]$P < 0.05$: Control *vs* sham; [c]$P < 0.05$: Control *vs* sleeve gastrectomy; [e]$P < 0.05$: Sham *vs* SG. ET: Endothelin; ECE: ET-converting enzyme; SG: Sleeve gastrectomy.

A

B

Figure 5 Immunohistochemical assessment of DNA damage using the γ-H2AX foci assay. A: Representative images of γ-H2AX-positive cells (red arrows) at different time points (bar = 20 μm); B: Semi-quantification of the level of DNA damage. [a]$P < 0.05$: Control *vs* sham; [c]$P < 0.05$: Sham *vs* sleeve gastrectomy. SG: sleeve gastrectomy.

ARTICLE HIGHLIGHTS

Research background

Although it is stated that bariatric surgeries are capable of preventing numerous types of cardiovascular diseases and cancer, the basic studies are still warranted to explain such roles by revealing the possible mechanisms. Herein, an attempt was made to answer these questions in an innovative way by investigating one of the important regulation systems in the body – the endothelin-1 (ET-1) axis.

Research motivation

Providing evidence for the lowered risk of cardiovascular disease and cancer will not only enlighten the multifunctional effects of sleeve gastrectomy (SG), which is deemed to be "metabolic", but also broaden and deepen our understanding of related fields and help improve the acceptance of SG as well.

Research objectives

In the current study, an ameliorated status of the ET-1 axis was confirmed, indicating the improvement in endothelial function and decline in the risk of lung cancer. Plus, the latter was also identified by the decreased level of DNA damage. Collectively, these findings are bound to attract and inspire future researchers to look for the clues of the benefits brought by bariatric surgeries that extend beyond the known metabolic improvements.

Research methods

SG and sham surgery were performed to clarify the effect induced on the ET-1 axis. In order to determine the real baseline of the parameters, healthy controls were also included. Moreover, the γ-H2AX foci assay was applied to provide stronger evidence of SG in preventing lung cancer, which was not an approach used commonly in previous research related to bariatric surgeries.

Research results

The results indicated that SG improved endothelial function and prevented lung cancer by normalizing the ET-1 axis, providing animal-based findings and suggesting new perspectives for the clinical field. The potential mechanisms of how SG effects the ET-1 axis and whether it is a direct impact or achieved by moderating metabolic disorder, however, need to be explored further.

Research conclusions

Beyond reducing body weight and improving both glycometabolism and insulin sensitivity, SG improves endothelial function and exerts a protective role in preventing lung cancer by normalizing the ET-1 axis and lessening DNA damage. These findings may present a new theoretical basis for clinical implications of SG.

Research perspectives

We believe that looking for more lines of evidence which expand our knowledge beyond the metabolic impact of bariatric surgeries is important, particularly because it will illuminate and illustrate the whole picture of the therapeutic effects of these procedures. Undoubtedly, factors that change under metabolic disorder and contribute to canceration, are the entry points and keys to the answer.

ACKNOWLEDGEMENTS

REFERENCES

1   **Wiseman M**. The second World Cancer Research Fund/American Institute for Cancer Research expert report. Food, nutrition, physical activity, and the prevention of cancer: a global perspective. *Proc Nutr Soc* 2008; **67**: 253-256 [PMID: 18452640 DOI: 10.1017/S002966510800712X]

2   **Pothuraju R**, Rachagani S, Junker WM, Chaudhary S, Saraswathi V, Kaur S, Batra SK. Pancreatic cancer associated with obesity and diabetes: an alternative approach for its targeting. *J Exp Clin Cancer Res* 2018; **37**: 319 [PMID: 30567565 DOI: 10.1186/s13046-018-0963-4]

3   **Doytcheva P**, Bächler T, Tarasco E, Marzolla V, Engeli M, Pellegrini G, Stivala S, Rohrer L, Tona F, Camici GG, Vanhoutte PM, Matter CM, Lutz TA, Lüscher TF, Osto E. Inhibition of Vascular c-Jun N-Terminal Kinase 2 Improves Obesity-Induced Endothelial Dysfunction After Roux-en-Y Gastric Bypass. *J Am Heart Assoc* 2017; 6 [PMID: 29138180 DOI: 10.1161/JAHA.117.006441]

4   **Sudhahar V**, Okur MN, Bagi Z, O'Bryan JP, Hay N, Makino A, Patel VS, Phillips SA, Stepp D, Ushio-Fukai M, Fukai T. Akt2 (Protein Kinase B Beta) Stabilizes ATP7A, a Copper Transporter for Extracellular Superoxide Dismutase, in Vascular Smooth Muscle: Novel Mechanism to Limit Endothelial Dysfunction in Type 2 Diabetes Mellitus. *Arterioscler Thromb Vasc Biol* 2018; **38**: 529-541 [PMID: 29301787 DOI: 10.1161/ATVBAHA.117.309819]

5   **Iglarz M**, Clozel M. Mechanisms of ET-1-induced endothelial dysfunction. *J Cardiovasc Pharmacol* 2007; **50**: 621-628 [PMID: 18091577 DOI: 10.1097/FJC.0b013e31813c6cc3]

6   **Rubanyi GM**, Polokoff MA. Endothelins: molecular biology, biochemistry, pharmacology, physiology, and pathophysiology. *Pharmacol Rev* 1994; **46**: 325-415 [PMID: 7831383 DOI: 10.2165/00019053-199406030-00009]

7   **Bagnato A**, Natali PG. Endothelin receptors as novel targets in tumor therapy. *J Transl Med* 2004; **2**: 16 [PMID: 15165288 DOI: 10.1186/1479-5876-2-16]

8   **Bagnato A**, Loizidou M, Pflug BR, Curwen J, Growcott J. Role of the endothelin axis and its antagonists in the treatment of cancer. *Br J Pharmacol* 2011; **163**: 220-233 [PMID: 21232046 DOI: 10.1111/j.1476-5381.2011.01217.x]

9   **Bhalla A**, Haque S, Taylor I, Winslet M, Loizidou M. Endothelin receptor antagonism and cancer. *Eur J Clin Invest* 2009; **39** Suppl 2: 74-77 [PMID: 19335749 DOI: 10.1111/j.1365-2362.2009.02123.x]

10   **Nelson J**, Bagnato A, Battistini B, Nisen P. The endothelin axis: emerging role in cancer. *Nat Rev Cancer* 2003; **3**: 110-116 [PMID: 12563310 DOI: 10.1038/nrc990]

11   **Inoue A**, Yanagisawa M, Kimura S, Kasuya Y, Miyauchi T, Goto K, Masaki T. The human endothelin family: three structurally and pharmacologically distinct isopeptides predicted by three separate genes. *Proc Natl Acad Sci USA* 1989; **86**: 2863-2867 [PMID: 2649896 DOI: 10.1073/pnas.86.8.2863]

12   **Russell FD**, Davenport AP. Secretory pathways in endothelin synthesis. *Br J Pharmacol* 1999; **126**: 391-398 [PMID: 10077230 DOI: 10.1038/sj.bjp.0702315]

13   **Namiki A**, Hirata Y, Ishikawa M, Moroi M, Aikawa J, Machii K. Endothelin-1- and endothelin-3-induced vasorelaxation via common generation of endothelium-derived nitric oxide. *Life Sci* 1992; **50**: 677-682 [PMID: 1738296 DOI: 10.1016/0024-3205(92)90470-a]

14   **Smollich M**, Wülfing P. The endothelin axis: a novel target for pharmacotherapy of female malignancies. *Curr Vasc Pharmacol* 2007; **5**: 239-248 [PMID: 17627567 DOI: 10.2174/157016107781024082]

15   **Bagnato A**, Rosanò L, Spinella F, Di Castro V, Tecce R, Natali PG. Endothelin B receptor blockade inhibits dynamics of cell interactions and communications in melanoma cell progression. *Cancer Res* 2004; **64**: 1436-1443 [PMID: 14973117 DOI: 10.1158/0008-5472.can-03-2344]

16   **Nelson J**. Endothelin Receptors as Therapeutic Targets in Castration-Resistant Prostate Cancer. *Eur Urol Suppl* 2009; **8**: 20-28 [DOI: 10.1016/j.eursup.2008.10.004]

17   **Moody TW**, Ramos-Alvarez I, Moreno P, Mantey SA, Ridnour L, Wink D, Jensen RT. Endothelin causes transactivation of the EGFR and HER2 in non-small cell lung cancer cells. *Peptides* 2017; **90**: 90-99 [PMID: 28153500 DOI: 10.1016/j.peptides.2017.01.012]

18   **Zhang WM**, Zhou J, Ye QJ. Endothelin-1 enhances proliferation of lung cancer cells by increasing intracellular free Ca2+. *Life Sci* 2008; **82**: 764-771 [PMID: 18294657 DOI: 10.1016/j.lfs.2008.01.008]

19   **Chen JL**, Lv XD, Ma H, Chen JR, Huang JA. Detection of cancer embryo antigen and endothelin-1 in exhaled breath condensate: A novel approach to investigate non-small cell lung cancer. *Mol Clin Oncol* 2016; **5**: 124-128 [PMID: 27330782 DOI: 10.3892/mco.2016.902]

20   **Dumanskiy YV**, Stoliarova OY, Syniachenko OV, Iegudina ED. Endothelial dysfunction of vessels at lung cancer. *Exp Oncol* 2015; **37**: 277-280 [PMID: 26710840 DOI: 10.31768/2312-8852.2015.37(4):277-280]

21   **Rogakou EP**, Pilch DR, Orr AH, Ivanova VS, Bonner WM. DNA double-stranded breaks induce histone H2AX phosphorylation on serine 139. *J Biol Chem* 1998; **273**: 5858-5868 [PMID: 9488723 DOI: 10.1074/jbc.273.10.5858]

22   **Varvara PV**, Karaolanis G, Valavanis C, Stanc G, Tzaida O, Trihia H, Patapis P, Dimitroulis D, Perrea D. gamma-H2AX: A potential biomarker in breast cancer. *Tumour Biol* 2019; **41**: 1010428319878536 [PMID: 31552812 DOI: 10.1177/1010428319878536]

23   **Zhao L**, Chang DW, Gong Y, Eng C, Wu X. Measurement of DNA damage in peripheral blood by the γ-H2AX assay as predictor of colorectal cancer risk. *DNA Repair (Amst)* 2017; **53**: 24-30 [PMID: 28291710 DOI: 10.1016/j.dnarep.2017.03.001]

24   **Ochola DO**, Sharif R, Bedford JS, Keefe TJ, Kato TA, Fallgren CM, Demant P, Costes SV, Weil MM. Persistence of Gamma-H2AX Foci in Bronchial Cells Correlates with Susceptibility to Radiation Associated Lung Cancer in Mice. *Radiat Res* 2019; **191**: 67-75 [PMID: 30398394 DOI: 10.1667/RR14979.1]

25   **Sjöström L**, Narbro K, Sjöström CD, Karason K, Larsson B, Wedel H, Lystig T, Sullivan M, Bouchard C, Carlsson B, Bengtsson C, Dahlgren S, Gummesson A, Jacobson P, Karlsson J, Lindroos AK, Lönroth H, Näslund I, Olbers T, Stenlöf K, Torgerson J, Agren G, Carlsson LM; Swedish Obese Subjects Study. Effects of bariatric surgery on mortality in Swedish obese subjects. *N Engl J Med* 2007; **357**: 741-752 [PMID: 17715408 DOI: 10.1056/NEJMoa066254]

26   **Schauer DP**, Feigelson HS, Koebnick C, Caan B, Weinmann S, Leonard AC, Powers JD, Yenumula PR, Arterburn DE. Bariatric Surgery and the Risk of Cancer in a Large Multisite Cohort. *Ann Surg* 2019; **269**: 95-101 [PMID: 28938270 DOI: 10.1097/SLA.0000000000002525]

27   **Anveden Å**, Taube M, Peltonen M, Jacobson P, Andersson-Assarsson JC, Sjöholm K, Svensson PA, Carlsson LMS. Long-term incidence of female-specific cancer after bariatric surgery or usual care in the Swedish Obese Subjects Study. *Gynecol Oncol* 2017; **145**: 224-229 [PMID: 28259424 DOI: 10.1016/j.ygyno.2017.02.036]

28   **Schauer DP**, Feigelson HS, Koebnick C, Caan B, Weinmann S, Leonard AC, Powers JD, Yenumula PR, Arterburn DE. Association Between Weight Loss and the Risk of Cancer after Bariatric Surgery. *Obesity (Silver Spring)* 2017; **25** Suppl 2: S52-S57 [PMID: 29086527 DOI: 10.1002/oby.22002]

29   **He R**, Yin Y, Yin W, Li Y, Zhao J, Zhang W. Prevention of pancreatic acinar cell carcinoma by Roux-en-Y Gastric Bypass Surgery. *Nat Commun* 2018; **9**: 4183 [PMID: 30305629 DOI: 10.1038/s41467-018-06571-w]

30   **Aravani A**, Downing A, Thomas JD, Lagergren J, Morris EJA, Hull MA. Obesity surgery and risk of colorectal and other obesity-related cancers: An English population-based cohort study. *Cancer Epidemiol* 2018; **53**: 99-104 [PMID: 29414638 DOI: 10.1016/j.canep.2018.01.002]

31   **Russell WS**, Burch RL. The Principles of Humane Experimental Technique. *Med J Australia* 1959; **1**: 500 [DOI: 10.5694/j.1326-5377.1960.tb73127.x]

32   **Sun D**, Liu S, Zhang G, Colonne P, Hu C, Han H, Li M, Hu S. Sub-sleeve gastrectomy achieves good diabetes control without weight loss in a non-obese diabetic rat model. *Surg Endosc* 2014; **28**: 1010-1018 [PMID: 24190081 DOI: 10.1007/s00464-013-3272-1]

33   **Matthews DR**, Hosker JP, Rudenski AS, Naylor BA, Treacher DF, Turner RC. Homeostasis model assessment: insulin resistance and beta-cell function from fasting plasma glucose and insulin concentrations in man. *Diabetologia* 1985; **28**: 412-419 [PMID: 3899825 DOI: 10.1007/bf00280883]

34   **Szmitko PE**, Wang CH, Weisel RD, de Almeida JR, Anderson TJ, Verma S. New markers of inflammation and endothelial cell activation: Part I. *Circulation* 2003; **108**: 1917-1923 [PMID: 14568885 DOI: 10.1161/01.Cir.0000089190.95415.9f]

35   **Engin A**. Endothelial Dysfunction in Obesity. *Adv Exp Med Biol* 2017; **960**: 345-379 [PMID: 28585207 DOI: 10.1007/978-3-319-48382-5_15]

36   **Dhananjayan R**, Koundinya KS, Malati T, Kutala VK. Endothelial Dysfunction in Type 2 Diabetes Mellitus. *Indian J Clin Biochem* 2016; **31**: 372-379 [PMID: 27605734 DOI: 10.1007/s12291-015-0516-y]

37   **van Harmelen V**, Eriksson A, Aström G, Wåhlén K, Näslund E, Karpe F, Frayn K, Olsson T, Andersson J, Rydén M, Arner P. Vascular peptide endothelin-1 links fat accumulation with alterations of visceral adipocyte lipolysis. *Diabetes* 2008; **57**: 378-386 [PMID: 18025413 DOI: 10.2337/db07-0893]

38   **Arner P**. Human fat cell lipolysis: biochemistry, regulation and clinical role. *Best Pract Res Clin Endocrinol Metab* 2005; **19**: 471-482 [PMID: 16311212 DOI: 10.1016/j.beem.2005.07.004]

39   **Quehenberger P**, Bierhaus A, Fasching P, Muellner C, Klevesath M, Hong M, Stier G, Sattler M, Schleicher E, Speiser W, Nawroth PP. Endothelin 1 transcription is controlled by nuclear factor-kappaB in AGE-stimulated cultured endothelial cells. *Diabetes* 2000; **49**: 1561-1570 [PMID: 10969841 DOI: 10.2337/diabetes.49.9.1561]

40   **Sármán B**, Tóth M, Somogyi A. Role of endothelin-1 in diabetes mellitus. *Diabetes Metab Rev* 1998; **14**: 171-175 [PMID: 9679669 DOI: 10.1002/(sici)1099-0895(199806)14:2<171::aid-dmr207>3.0.co;2-g]

41   **Irani S**, Salajegheh A, Smith RA, Lam AK. A review of the profile of endothelin axis in cancer and its management. *Crit Rev Oncol Hematol* 2014; **89**: 314-321 [PMID: 24035584 DOI: 10.1016/j.critrevonc.2013.08.011]

42   **Ahmed SI**, Thompson J, Coulson JM, Woll PJ. Studies on the expression of endothelin, its receptor subtypes, and converting enzymes in lung cancer and in human bronchial epithelium. *Am J Respir Cell Mol Biol* 2000; **22**: 422-431 [PMID: 10745023 DOI: 10.1165/ajrcmb.22.4.3795]

43   **Gohji K**, Kitazawa S, Tamada H, Katsuoka Y, Nakajima M. Expression of endothelin receptor a associated with prostate cancer progression. *J Urol* 2001; **165**: 1033-1036 [PMID: 11176535 DOI:

10.1016/S0022-5347(05)66597-4]

44   **Wülfing P**, Diallo R, Kersting C, Wülfing C, Poremba C, Rody A, Greb RR, Böcker W, Kiesel L. Expression of endothelin-1, endothelin-A, and endothelin-B receptor in human breast cancer and correlation with long-term follow-up. *Clin Cancer Res* 2003; **9**: 4125-4131 [PMID: 14519635 DOI: 10.1002/cncr.11592]

45   **Kedzierski RM**, Yanagisawa M. Endothelin system: the double-edged sword in health and disease. *Annu Rev Pharmacol Toxicol* 2001; **41**: 851-876 [PMID: 11264479 DOI: 10.1146/annurev.pharmtox.41.1.851]

46   **Jenkins HN**, Williams LJ, Dungey A, Vick KD, Grayson BE, Speed JS. Elevated plasma endothelin-1 is associated with reduced weight loss post vertical sleeve gastrectomy. *Surg Obes Relat Dis* 2019; **15**: 1044-1050 [PMID: 31147283 DOI: 10.1016/j.soard.2019.03.047]

47   **Pontiroli AE**, Pizzocri P, Koprivec D, Vedani P, Marchi M, Arcelloni C, Paroni R, Esposito K, Giugliano D. Body weight and glucose metabolism have a different effect on circulating levels of ICAM-1, E-selectin, and endothelin-1 in humans. *Eur J Endocrinol* 2004; **150**: 195-200 [PMID: 14763917 DOI: 10.1530/eje.0.1500195]

48   **Irigaray P**, Belpomme D. Basic properties and molecular mechanisms of exogenous chemical carcinogens. *Carcinogenesis* 2010; **31**: 135-148 [PMID: 19858070 DOI: 10.1093/carcin/bgp252]

49   **Wlodarczyk M**, Nowicka G. Obesity, DNA Damage, and Development of Obesity-Related Diseases. *Int J Mol Sci* 2019; 20 [PMID: 30845725 DOI: 10.3390/ijms20051146]

50   **Minamino T**, Orimo M, Shimizu I, Kunieda T, Yokoyama M, Ito T, Nojima A, Nabetani A, Oike Y, Matsubara H, Ishikawa F, Komuro I. A crucial role for adipose tissue p53 in the regulation of insulin resistance. *Nat Med* 2009; **15**: 1082-1087 [PMID: 19718037 DOI: 10.1038/nm.2014]

51   **Hinault C**, Kawamori D, Liew CW, Maier B, Hu J, Keller SR, Mirmira RG, Scrable H, Kulkarni RN. Δ40 Isoform of p53 controls β-cell proliferation and glucose homeostasis in mice. *Diabetes* 2011; **60**: 1210-1222 [PMID: 21357466 DOI: 10.2337/db09-1379]

52   **Lee SC**, Chan JC. Evidence for DNA damage as a biological link between diabetes and cancer. *Chin Med J (Engl)* 2015; **128**: 1543-1548 [PMID: 26021514 DOI: 10.4103/0366-6999.157693]

53   **Blanco D**, Vicent S, Fraga MF, Fernandez-Garcia I, Freire J, Lujambio A, Esteller M, Ortiz-de-Solorzano C, Pio R, Lecanda F, Montuenga LM. Molecular analysis of a multistep lung cancer model induced by chronic inflammation reveals epigenetic regulation of p16 and activation of the DNA damage response pathway. *Neoplasia* 2007; **9**: 840-852 [PMID: 17971904 DOI: 10.1593/neo.07517]

54   **Giovannini C**, Piaggi S, Federico G, Scarpato R. High levels of γ-H2AX foci and cell membrane oxidation in adolescents with type 1 diabetes. *Mutat Res* 2014; **770**: 128-135 [PMID: 25771879 DOI: 10.1016/j.mrfmmm.2014.08.005]

55   **Azzarà A**, Chiaramonte A, Filomeni E, Pinto B, Mazzoni S, Piaggi S, Angela Guzzardi M, Bruschi F, Iozzo P, Scarpato R. Increased level of DNA damage in some organs of obese Zucker rats by γ-H2AX analysis. *Environ Mol Mutagen* 2017; **58**: 477-484 [PMID: 28714549 DOI: 10.1002/em.22115]

56   **Lee YS**, Doonan BB, Wu JM, Hsieh TC. Combined metformin and resveratrol confers protection against UVC-induced DNA damage in A549 lung cancer cells via modulation of cell cycle checkpoints and DNA repair. *Oncol Rep* 2016; **35**: 3735-3741 [PMID: 27109601 DOI: 10.3892/or.2016.4740]

57   **Bankoglu EE**, Seyfried F, Arnold C, Soliman A, Jurowich C, Germer CT, Otto C, Stopper H. Reduction of DNA damage in peripheral lymphocytes of obese patients after bariatric surgery-mediated weight loss. *Mutagenesis* 2018; **33**: 61-67 [PMID: 29294093 DOI: 10.1093/mutage/gex040]

58   **Mitterberger MC**, Mattesich M, Zwerschke W. Bariatric surgery and diet-induced long-term caloric restriction protect subcutaneous adipose-derived stromal/progenitor cells and prolong their life span in formerly obese humans. *Exp Gerontol* 2014; **56**: 106-113 [PMID: 24747059 DOI: 10.1016/j.exger.2014.03.030]

59   **Bankoglu EE**, Seyfried F, Rotzinger L, Nordbeck A, Corteville C, Jurowich C, Germer CT, Otto C, Stopper H. Impact of weight loss induced by gastric bypass or caloric restriction on oxidative stress and genomic damage in obese Zucker rats. *Free Radic Biol Med* 2016; **94**: 208-217 [PMID: 26939878 DOI: 10.1016/j.freeradbiomed.2016.02.033]

Baishideng®